THE JOURNAL OF PHYSICAL CHEMISTRY C

ARTICLE

pubs.acs.org/JPCC

Structural and Electrical Properties of Flip Chip Laminated Metal−Molecule−Silicon Structures Varying Molecular Backbone and Atomic Tether

Mariona Coll,[†] Nadine Gergel-Hackett,[‡] Curt A. Richter, and Christina A. Hacker*

Semiconductor Electronics Division, Physical Measurement Laboratory, National Institute of Standards and Technology, Gaithersburg, Maryland 20899, United States

Supporting Information

ABSTRACT: Formation of electrical contacts to organic molecules by using a scalable technique that preserves molecular integrity is a key development toward reliable fabrication of nanoscale molecular architectures. Here we report the structural and electrical properties of metal−monolayer−silicon junctions fabricated by using Flip Chip Lamination (FCL), a novel, low cost, and nondestructive approach. The effect of junction formation is studied with both aliphatic and aromatic molecular backbones. The ω-functionalized monolayers are first formed on ultrasmooth gold via a thiol linkage and then laminated to H−Si via a thiol or alkene linkage. The application of pressure and temperature enables formation of the nanoscale molecular junctions chemically tethered to two electrodes. The molecular structure and interfacial chemistry within the electrical structure are investigated by using polarized backside-reflection absorption infrared spectroscopy (pb-RAIRS) and current−voltage (I−V) measurements. The confined organic monolayers maintain an overall structure similar to the original self-assembled monolayers (SAMs) on gold with small changes in the configuration of the molecular backbone attributed to lamination and bonding of the molecular terminal group to silicon and exhibiting electrical dielectric integrity. The optimal lamination conditions for each monolayer are dependent on the surface free energy, monolayer conformation, ambient conditions, and reaction of the molecular functionality with the silicon substrate. We demonstrate the structural and electrical integrity at the monolayer level of a variety of organic molecules bonded to both silicon and metal electrodes by probing the effect of molecular backbone (aliphatic vs aromatic) and molecule−electrode interface. FCL enables formation of an extended variety of molecular junctions to identify the critical factors in charge transport across metal−molecule−silicon nanoelectronic architectures.

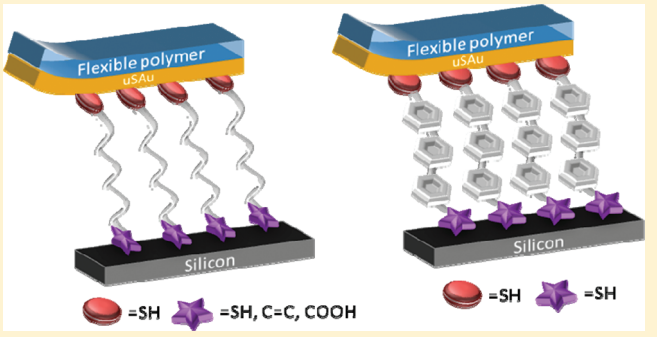

INTRODUCTION

Organic materials are highly attractive as active electronic components for many technological applications such as next generation memory and logic devices,[1] organic photovoltaics,[2] organic field-effect transistors,[3] or biosensors.[4] In particular, the concept of combining organic molecules with conventional silicon technology has galvanized the molecular electronics field.[5] Silicon is an ideal platform for molecule-based devices offering the fabrication and operational foundation from the microelectronics industry to facilitate novel molecule-dependent nanoscale designs and applications. The use of metal−molecule−silicon (MMS) structures rather than metal−molecule−metal (MMM) allows the opportunity to integrate with existing microelectronics and combine semiconducting function with molecular architectures to make unique electrical components. For example, the prospect of combining the semiconductor properties of silicon with organic molecules has been proposed for possible applications in logic and low-power memory.[6] Ultimately, it is desirable to fabricate molecular junctions with a large variety of organic molecules incorporating different chemistries and properties providing potential new functionalities.

Historically, the fabrication of reliable molecular electronic structures has proven difficult due to several factors including (1) electrode surface roughness; (2) molecule−electrode chemistry; (3) molecular geometry within the organic thin film; (4) structure, packing, and orientation variations within the monolayer; and (5) electrode deposition methods.[5b,d,7] For thin-film applications, fabrication is usually approached through optimization of the three individual components: bottom electrode, molecular layer, and top electrode. To achieve reliable structures on the nanometer length scale, the bottom electrode must be as close to atomically smooth as possible with few contributions from defects, steps, grain boundaries, or other topology. The smoothness aids formation of uniform monolayers which maximize intermolecular forces while having few defects for metal penetration. Also, roughness variations within a nanoscale molecular junction can have a large effect on the electrical results due to the exponential

Received: August 26, 2011
Revised: October 18, 2011
Published: October 19, 2011

ACS Publications This article not subject to U.S. Copyright. Published 2011 by the American Chemical Society

length dependence[8] of tunneling-related conduction mechanisms. Ultrasmooth bottom electrode surfaces have been made by utilizing pyrolyzed photoresist,[9] template stripped metals,[10] or Au deposition on molecular modified substrates.[11] The hydrogen-terminated silicon (111) surface can be made very smooth by removal of the oxide layer with buffered hydrofluoric acid.[12]

Monolayer formation on the optimized electrode surface presents an additional set of challenges. Formation of high-quality monolayers requires a balance of molecule−electrode and molecule−molecule interactions. The electrode−molecule interface plays a critical role in the ensemble MMS electrical properties since it can lead to different bond strength and a different degree of coupling between molecule and electrode[13] and it can present interface dipoles[14] that alter charge transport in the molecular junction. Also, molecular topology or molecular conformation, which sometimes is imposed by the bond with the electrode, can affect transport properties.[15] For most materials, the coupling of molecules must also provide good chemical resistance to prevent further reaction/oxidation of the interface. For semiconductors, which are known to have electrically active semiconductor interfacial states, the molecular layer must also provide electrical passivation.[16] Previous studies of monolayers on GaAs have highlighted a trade-off between intermolecular forces and interfacial forces where dense molecular layers (seemingly optimized intermolecular properties) generate interfacial defect traps (poor interfacial forces).[17] Monolayers on silicon, a surface where neither the adsorbate nor the semiconductor atoms have much surface mobility due to strong covalent bonding, are often poorly ordered[18] compared with gold−thiol[19] self-assembled monolayers. However, the molecular layers on silicon are tethered by strong covalent bonds that facilitate junction robustness and maintain high electrical quality.[20] To date, the complexity in forming monolayers from bifunctional molecules on silicon substrates[21] has limited the study of MMS junctions to mainly aliphatic molecules with Si−C or Si−O−C interfaces.[5d,20c,22] The formation of aromatic monolayers with diazonium chemistry leading to Si−C bonding is an alternate route with mixed results reported for molecules containing a second functional group and difficulty limiting the molecular functionalization to one monolayer.[23]

Making electrical contact to organic molecules and verifying the molecular structure within the junction remains one of the most pivotal challenges in this field.[5d,7,24] Conventional metal vapor deposition techniques often lead to electrical shorts and disrupt the molecular order.[20b,22b,23b,25] Early efforts found limited success with intentional use of terminal functional groups to interact with vapor-deposited metal to impede damaging the molecular layer and filament formation.[25d,26] More recent approaches have successfully reported formation of molecular junctions maintaining structural and electronic integrity by using "soft metallization" efforts to form the top electrical contact including Hg drop,[27] indirect metallization,[23b,28] placement of preformed metal pads,[23b,28,29] or Flip Chip Lamination (FCL).[10a,24c,30] Verifying the integrity of the molecules under a top electrode is often challenging as electrically conducting top electrodes are typically opaque to most optical and spectroscopic characterization techniques. Often the monolayer structure is inferred from semitransparent electrodes or destructive sampling techniques. Fortunately, silicon is transparent in the infrared, thus backside reflection absorption infrared spectroscopy has been used to characterize fully formed molecular junctions providing structural information to directly correlate with electrical data.[20b,22b,23b]

We have previously demonstrated flip chip lamination as an approach to build molecular junctions in such a way as to overcome many of the typical fabrication challenges. This soft electrode deposition method utilizes ω-functionalized SAMs formed through Au−S chemistry to uniformly adhere to the second electrode, in this case silicon, forming reliable molecular junctions with less defective monolayers and more reproducible electrical junctions than those obtained with conventional metallization. This approach relies on an ultrasmooth gold surface with minimal roughness to ensure the self-assembling molecules can maximize van der Waals and surface interactions to create a dense monolayer with fewer defects and grain boundaries while presenting a relatively homogeneous top surface for bonding to the second electrode.[31] The density and orientation of molecular groups reacting with the second electrode surface is largely determined by the gold−thiol self-assembly. Second, the ultrasmooth gold electrode is adhered to a flexible substrate which is necessary for uniform nanotransfer printing (nTP) of the Au monolayer to the silicon surface under solvent-free conditions. Attempts to bond preformed organic molecules on Si under solvent-free and under thermomechanical conditions are rather limited. Thus, the reaction mechanism and interface structure of these Si−molecule−Au junctions is, in many cases, unknown, making the control of monolayer lamination to the H−Si surface a key challenge. Direct coupling between the functional molecular groups and the H−Si surface in FCL differs substantially from the traditional adsorption mechanisms as the physical and chemical environments of the preformed monolayer largely determine the interfacial reactivity. Therefore, monolayer lamination in this study is investigated for several thiol molecules with different functional end group chemistry and molecular backbone to achieve molecular anchoring to the silicon surface. Thus, the use of a fabrication technique such as FCL is highly advantageous not only for the formation of reliable monolayer scale junctions but also for the versatility to form MMS structures from a variety of molecular layers and electrode materials.

In this work, we utilize the FCL fabrication paradigm to investigate formation of MMS junctions with differing molecular backbone and interfacial chemistry. We investigate FCL preparation of molecular junctions from aliphatic alkene-terminated alkanethiols (mercaptohexadecene, MHE), decanedithiols (DDT), and aromatic terphenyldithiols (TPDT), with comparison to mercaptohexadecanoic acid (MHA) junctions discussed in earlier work,[10a] as shown in Scheme 1. Ordered and densely packed ω-functionalized thiol monolayers are obtained by self-assembly through the Au−S bond and characterized by using reflection absorption infrared spectroscopy (RAIRS), contact angle goniometry (CA), spectroscopic ellipsometry (SE), and X-ray photoelectron spectroscopy (XPS). These bifunctional monolayers on uSAu are flipped and pressed onto an H-terminated silicon substrate (H−Si) to form metal−molecule−Si junctions with conformal contact facilitated by the flexible substrate under ultrasmooth gold. After lamination, the interfacial bonding and molecular structure of the buried monolayer can be characterized by using nondestructive *p*-polarized backside reflection absorption infrared spectroscopy (pb-RAIRS), taking advantage of the infrared transparent nature of silicon.[20b,32] This enables the same architecture to be used to perform the structural and electrical characterization, allowing direct correlation between the organic structure and the electrical function. Thorough analyses of the monolayers within the MMS junction highlight the relevant mechanism for monolayer lamination and the molecular changes

Scheme 1. (a) Schematic of the FCL Generated Nanoelectronic Architecture with Molecular Junctions Chemically Bonded to Ultrasmooth Au (usAu) and Silicon Electrodes and (b) Molecular Structure of Starting Materials[a]

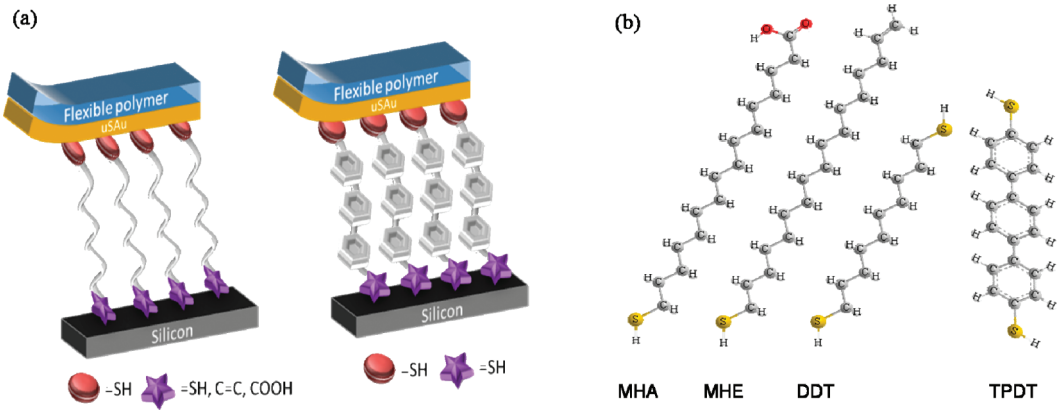

[a] MHA, mercaptohexadecanoic acid; MHE, mercaptohexadecene; DDT, decanedithiol; and TPDT, *p*-terphenyldithiol.

induced by lamination to silicon. FCL is a versatile and nondestructive fabrication route to form reliable nanoscale molecular architectures and offers a valuable addition to the "soft metallization" repertoire.

EXPERIMENTAL MATERIALS AND METHODS

Monolayer Formation. All chemicals purchased are ACS grade (CH_2═$CH-(CH_2)_{14}-SH$ (MHE); $SH-(CH_2)_{10}-SH$ (DDT); $HS-(C_6H_4)_3-SH$ (TPDT)) and used as received. Preparation of uSAu/PET substrates was performed by e-beam evaporation of 100 nm of Au on a silicon substrate previously treated with a fluorinated silane F1 (tridecafluoro-1,1,2,2,-tetrahydro-octyltrichlorosilane). The large area junctions prepared for infrared characterization were generated by placing a PET substrate in contact with the Au and placed within the nanoTransfer printing (nTP) tool to release the Au from the SiO_2 substrate and expose the smooth surface on a flexible substrate. For the small area electrical measurements, a second fluorinated thiol F2 (3,3,4,4,5,5,6,6,7,7,8,8,8-tridecafluoro-octanethiol) release layer was used to further decrease the surface free energy of the gold surface. The Au/F1/SiO_2 substrate was immersed into an ethanolic solution of F2, rinsed with ethanol, and dried in nitrogen. Finally, the PET flexible substrate was placed in contact with the F2−Au/F1−Si substrate and placed within the nanoTransfer Printing (nTP) tool. Nanotransfer printing conditions were carefully optimized to facilitate the PET release after FCL and enable electrical contact to the Au electrode to perform electrical transport measurements. The uSAu/PET were cut in pieces of 1 cm × 1 cm and cleaned by consecutive ultraviolet−ozone (UV−O_3) exposure followed by deionized water and ethanol rinsing, and then they were dried with streaming nitrogen. Toluene-based solutions of 2 mM MHE and ethanolic solutions of 10 mM DDT and <1 mM TPDT were all prepared in a nitrogen-filled glovebox to minimize molecule oxidation. The low solubility of TPDT in ethanol required 30−45 min sonication followed by heating to 50 °C for 20 min to aid dissolution. For DDT and TPDT, uSAu/PET substrates were kept in solution for 4 h to minimize film polymerization (S−S bond formation).[33] For MHE formation, uSAu/PET substrates were kept in solution overnight. Following monolayer formation, the samples were rinsed with ethanol and isopropanol and dried with N_2 gas. Immediately after rinsing and drying, films were characterized to minimize monolayer degradation. Flip-chip lamination of self-assembled monolayers on double-side polished H−Si(111) has been optimized for each organic monolayer following a previously described process.[10a] Lamination temperature (35−120 °C),[34] pressure (0.5−2.8 MPa), and time (5−15 min) were optimized based on the structural properties and electrical response of the confined monolayer. Successful lamination was identified as occurring when the Au monolayer remained adhered to the silicon and the flexible PET could be peeled off and the integrity of the device maintained.

Structural characterization of the free-standing and FCL monolayer was evaluated by Fourier transform infrared spectroscopy (FTIR) performed by using a commercial Fourier transform infrared spectrometer with a liquid-nitrogen cooled mercury cadmium telluride (MCT) detector (600−4000 cm^{-1}) set to 8 cm^{-1} resolution. The angle of incidence was 70° from the surface normal. Freshly cleaned usAu/PET and e-beam evaporated Au/H−Si were used as references for freestanding monolayers and FCL samples, respectively.

Water Contact Angle (CA) measurements were performed at ambient conditions by using a custom tool. A drop of deionized water (18 MΩ·cm) was deposited on the monolayer surface, captured by a video camera, and stored on a computer. Commercial software was used to extract the contact angle values. This measurement was performed at least three times on each sample.

Spectroscopic ellipsometry measurements were performed on a commercial instrument with the angle of incidence set at 70° from the surface normal. Experimental data were fit using a Au/monolayer/air model where the optical properties of the monolayer were modeled as a Cauchy dispersion using n = 1.5. A monolayer of octadecanethiol (ODT) on uSAu/PET was used as a gold reference assuming a 2.3 nm thickness and n = 1.5.

X-ray photoelectron spectroscopy (XPS) measurements were performed with a commercial instrument equipped with a monochromatic Al Kα source (1486 KeV). Spectra were recorded at a nominal collection angle aligned with the surface normal with pass energy of 20 eV for the high-resolution C 1s, Au 4f, O 1s, and S 2p regions and 160 eV for the survey spectra.

Electrical measurements consisting of two terminal current−voltage measurements were acquired by using a commercial

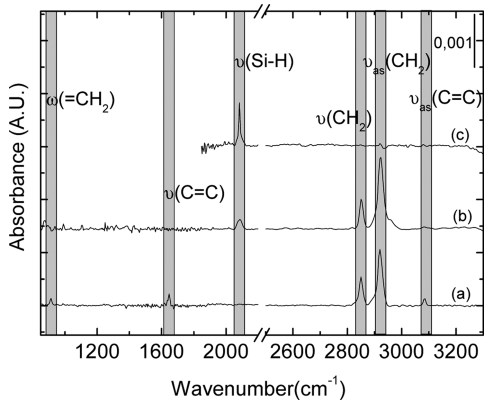

Figure 1. Reflection absorption spectrum of (a) free-standing MHE on uSAu/PET and a pb-RAIRS spectrum of (b) the FCL created junction consisting of Si-MHE-uSAu/PET. (c) A characteristic reflection absorption spectrum of Au on H−Si.

probe station under nitrogen and in the dark on patterned FCL uSAu/monolayer/Si structures with a device area of 1.76×10^{-4} cm^2. The FCL process yield for MHE and DDT was 100% and for TPDT > 90% as indicated by the number of structures transferred from the PET to the silicon. For each FCL molecule, at least 30 devices in two different runs were measured with an electrical yield of ≈90%. A metallic probe on freshly etched H−Si(111) was used to acquire control data. To avoid complications with the Schottky barrier and thus maximize the contribution of the monolayer on the electrical response, in these measurements n-type Si(111) substrates with $\rho = 0.001-0.005\ \Omega \cdot$cm were chosen.[10a,14f] To evaluate subtle differences between molecular layers, we have studied the current density histograms of all measured devices. Overall, the electrical results are remarkably consistent for a monolayer junction and present a small distribution of conductivities. The variation between fabrication runs (≈20% standard deviation) is larger than the variation of devices made in the same fabrication run (≈15% standard deviation). It is important to note that the variation in our results is similar to the variation reported in previous nanotransfer printing methods.[24b]

RESULTS AND DISCUSSION

MHE Monolayer Structure within the MMS Junction. The effect of junction formation on the structural properties of the free-standing MHE monolayer is shown in the vibrational spectra of Figure 1. Free-standing MHE monolayers assembled on uSAu/PET (Figure 1a) exhibit the characteristic methylene stretching vibrations $\upsilon_{as}(CH_2)$ at ≈2920 cm^{-1} and $\upsilon(CH_2)$ at ≈2850 cm^{-1} indicative of all-*trans* oriented monolayers.[35] Bands associated with the C═C functional group are observed at 3082, 1645, and 908 cm^{-1} assigned to $\upsilon_a(=CH_2)$, $\upsilon(C=C)$, and $\omega(=CH_2)$, respectively.[36] Lamination of the MHE monolayer to H−Si(111) under 0.5 MPa and 100 °C yields a bonded molecular junction as evidenced by the pb-RAIRS spectrum shown in Figure 1b. Within the MMS structure, the $\upsilon_{as}(CH_2)$ peak frequency shifts to ≈2922 cm^{-1}, and the absorbance intensity increases slightly, suggesting rearrangement of the MHE backbone alkyl chain while maintaining a relatively closely packed monolayer. The absence of soft CH_2 modes usually observed near ≈2858 cm^{-1} confirms no observable metal penetration[10a,20b] within the IR spectra of the alkyl backbone

Table 1. Spectroscopic Ellipsometric Thickness and Water Contact Angle Data for Free-Standing ODT, MHE, DDT, and TPDT Self-Assembled Monolayers on Au

SAM	SE (nm) ± 0.2 (nm)	CA_{H2O} (°) ± 2 (°)
ODT	2.3	108
MHE	2.4	90
DDT	1.2	70
TPDT	1.2	72

verifying FCL is a soft method to metalize delicate nanoscale structures.

Examination of infrared spectral features attributed to the alkene and Si−H surface can provide more insight into the nature of the molecular bonding with the silicon surface during lamination. The vibrational spectra of the free-standing MHE monolayer assembled on uSAu/PET are consistent with the previously observed tilt and twist (see Supporting Information). Furthermore, the SE thickness (see Table 1) of 2.4 nm ± 0.2 nm is consistent with a single monolayer. The water contact angle of 90° ± 2° differs from the expected value of hydrophobic alkene-terminated thiol adsorbed on Au (i.e., CA ≈ 107° for C19 alkene-thiol).[31] Small differences in CA are typically indicative of the terminal functional group density and orientation and vary with slight differences in molecular packing, surface roughness, and chain length. Rotation of the terminal alkene group induces some variability in chain conformation and is expected to influence chemical interactions with the H−Si(111) and resulting chain reorganization.

After lamination, the integrated intensity of the $\upsilon_a(=CH_2)$ mode at 3082 cm^{-1} is decreased by ≈40%. The $\upsilon(C=C)$ and $\omega(=CH_2)$ modes at 1645 and 908 cm^{-1}, respectively, can barely be identified after lamination as seen in Figure 1b. The decrease in olefin peaks can arise from a change in the C═C orientation due to the molecular reorientation or from reaction with the Si−H surface which is expected during lamination. Molecular reorientation estimated from the FTIR data indicates the chain tilt increase is approximately 15°, and there is a random heterogeneous twist (see Supporting Information). The IR metal surface selection rule[37] dictates that only modes perpendicular to the metal surface are observed, and the $\upsilon_a(=CH_2)$ and $\upsilon(C=C)$ modes have orthogonal transition dipole moments;[36] thus, changes in olefin group orientation would cause one mode to be more intense and the other to decrease. The observation that all olefin-related modes decrease in intensity suggests there is consumption of the alkene functionality during bonding, while minimal reorientation is likely.

The pb-RAIRS data of the FCL junction also show the presence of a broad $\upsilon(Si-H)$ peak identified at 2083 cm^{-1} at the semiconductor interface. A reference spectrum obtained from freshly etched H-terminated silicon is characterized by a sharp Si−H mode at ≈2083 cm^{-1}, shown in Figure 1c, indicative of atomically smooth and fully H-terminated Si(111).[38] The origin of small Si−H peak variations is particularly difficult since a variety of parameters such as surface roughening, contamination, partial oxidation/hydrogenation, or chemical interaction with the monolayer terminus can give rise to these features.[12a,39] Fitting of the $\upsilon(Si-H)$ peak area in the FCL Si−MHE−uSAu spectrum indicates the area is ≈30% less than the corresponding Au/Si−H spectrum. The disruption of the Si−H skeleton is tentatively assigned to the consumption of H−Si bonds during

lamination, consistent with the decrease in integrated area detected in C═C related modes. The absence of strong silicon oxide bands in the 1000−1100 cm^{-1} region supports the formation of a chemically tethered molecular junction with negligible silicon oxidation.[10a,34,39,40] The weak dipole moment of the Si−C mode at 678 cm^{-1} and its proximity to the strong Si phonon mode hinders the observation of this mode in the IR spectra.[41] Saturated alkyl monolayers on H−Si(111) from solution typically report a coverage lower than 50%[40,42] of the surface silicon atoms due to lattice mismatch and steric hindrances between alkyl chains, with the exception of methyl termination where 100% surface coverage can be obtained.[39,40] Within the FCL process, preformed monolayers are brought into contact with the H−Si surface in a process where the molecular density and functional group availability have been determined by the self-assembly on the ultrasmooth Au surface. Thus, the estimated reactivity of MHE and H−Si obtained during lamination is in reasonable agreement with the reactivity observed for alkene assembly on H-terminated silicon substrates.

The reaction of ω-functionalized monolayers with the H−Si(111) surface in FCL differs from previous solution-based reports of monolayers on silicon since the FCL fabrication process brings an already formed ω-functionalized monolayer into contact with H−Si(111) without solution under applied pressure and temperature. Molecular conformation of SAMs on Au, chain rigidity, and interchain interactions can influence the accessibility of the functional end group to react with H−Si. Recent FCL studies of carboxy-terminated monolayers on gold showed successful lamination to the H−Si(111) substrate under mild conditions of pressure (0.8 MPa) and under a broad temperature range (30−110 °C).[10a,34] In the case of alkene-terminated monolayers described here, interaction with the H−Si(111) surface is observed under slightly different conditions, 0.5 MPa and $T \approx$ 100 °C. The reactivity of alkene and carboxy groups with H−Si(111) has been evaluated by theoretical calculations[43] and experimentally explored under a variety of conditions, including thermal and photochemical activation.[41a,44] The reaction mechanism in each case depends on the initial reaction conditions and is still under discussion. Interestingly, previous solution-based reports of bifunctional molecules containing both alkene and carboxy groups (i.e., undecylenic acid) with H−Si(111) observed bonding preferentially occurs through the alkene terminus.[44a] Since FCL utilizes monolayers that are preformed, surface parameters such as contact area or surface free energy likely affect the interfacial reaction.[43,45] MHE and MHA have the same molecular chain length and alkyl backbone, both adopting an all-trans *zig-zag* conformation when self-assembled on Au substrates, differing only in the terminal functional group.[10a,36,46] The carboxylic acid groups produce a hydrophilic surface with $CA_{H2O} \approx 10°$ and can establish hydrogen-bonding networks among neighboring molecules.[47] In contrast, alkene-terminated monolayers exhibit a highly hydrophobic surface with a $CA_{H2O} > 90°$ routinely observed in this study.[31] The contact angle of SAMs can be correlated with the work of adhesion (W_a) described by the Young−Dupre eq 1, as follows[48]

$$W_a = \gamma_{la}(1 + \cos\theta) \quad (1)$$

where γ_{la} is the surface tension and θ the water contact angle. Thus, the dissimilarities in surface free energies of the SAMs would indicate more energy is needed to adhere to the alkene-terminated SAM and could be responsible for the different experimental conditions needed to interact with H−Si(111). Intimate contact between the alkene functional group and the H−Si surface could be readily achieved based on their hydrophobic nature; however, temperatures ≈100 °C and 0.5 MPa are required to adhere the alkene functionality to H−Si(111). The applied pressure in FCL is unlikely to lead to significant adhesion between the alkene functional group and the H−Si(111) surface or conformational disorder within the aliphatic backbone, as much higher pressures are needed to irreversibly modify alkanethiol chains.[10a,49] The applied temperature needed for junction formation could have a dual role in lamination. The reaction can be thermally activated by activating H−Si bonds to create surface dangling bonds.[50] Simultaneously temperature-induced conformational changes in the monolayer terminus, consistent with the changes observed at the pb-RAIRS spectra and depicted in Scheme S1 (Supporting Information), would favor reaction of the alkene and H−Si surface by bringing the C_β closer to H−Si to potentially abstract hydrogen from a nearby surface silicon atom to create more reactive sites.

FCL of carboxy-terminated monolayers to H−Si was achievable at lower temperatures ($T \approx 30$ °C up to 100 °C) and failed at higher temperatures $T > 110$ °C.[34] Since the samples are prepared in air, the hydrophilic COOH-terminated monolayers are expected to contain a hydration layer which may modify interface reactivity. On the basis of Monte Carlo simulations, water molecules can be present as isolated clusters at low humidity and can form two to five monolayers at higher humidity.[51] Previous reports have pointed out the strong dependence of surface friction and adhesion on humidity, particularly for hydrophilic surfaces.[52] For example, adhesion between a Si_3N_4 scanning probe tip and a SiO_2 surface increased by a factor of 2 when the relative humidity increased from ≈25% to ≈70%.[52b] Assuming the average relative humidity in the laboratory at 25 °C is around 50%, it is consistent to expect a discrete hydration layer on the carboxy-terminated monolayers mediating the adhesion. Poor adhesion at higher temperatures may be linked to the disruption of the hydration layer which mediates attachment of the carboxyl group with the silicon surface.

FCL can create MHE monolayers between Au and Si electrodes maintaining an all-*trans* conformation and preventing silicon oxidation and Au penetration. Interfacial adhesion of well-ordered long-chain ω-functionalized monolayers to H−Si(111) depends strongly on the chemistry of the functional end group (i.e., COOH vs C═C), ambient humidity, and external conditions such as lamination temperature. To demonstrate the potential of this FCL approach, it is appealing to study molecules with other functional end groups such as thiols (−SH) and also different chain length and organic backbones.

Dithiol Monolayer Structure Within the MMS Junction. The attachment of alkyl molecules to Si(111) through a thiol tether is less studied compared to other moieties such as silanes,[53] alkenes,[44b,50,54] or alcohols.[20c,40] We have investigated the formation of Si−thiol molecular juctions from decanedithiol (DDT) monolayers on gold. Prior work reported the complexity in forming ordered and "standing-up" monolayers of dithiols maintaining unreacted −SH end groups.[33,55] Both thiol end groups can react with the Au surface and with other molecules forming structures where the molecules are "laying-down" on the surface or "looped" on the surface where both thiols are bonded but the aliphatic backbone is not in contact with the surface and multilayers where the molecules are linked through disulfide or sulfoxy bonds. Reflection absorption spectra of free-standing DDT monolayers

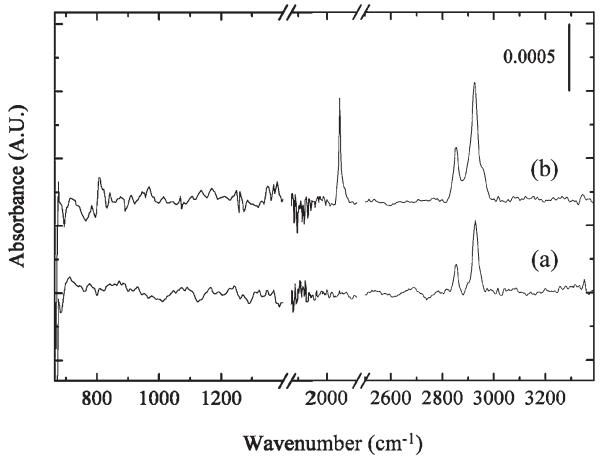

Figure 2. Reflection absorption spectrum of (a) free-standing DDT on uSAu/PET and (b) the pb-RAIRS spectrum of the FCL fabricated the uSAu−DDT−Si junction.

on gold present a $\upsilon_{as}(CH_2)$ located at 2927 cm^{-1}, shown in Figure 2a, indicating the aliphatic backbone exhibits a liquid-like structure indicative of little aliphatic chain ordering, as expected for a short alkyl chain length and consistent with previous studies.[56] The measured SE thickness of 1.2 nm and water contact angle of ≈70° (Table 1) confirm the formation of a monolayer with most of the −SH groups exposed at the air surface.[57] XPS analysis (see Supporting Information) corroborates the presence of a DDT monolayer with little contribution of multilayer formation and a lower packing density than the reference octadecanethiol on gold (ODT/Au). Upon lamination at 90 °C and 2.8 MPa, the $\upsilon_{as}(CH_2)$ shifts to 2924 cm^{-1} with a slight increase in the absorbance intensity, shown in Figure 2b. This shift in peak frequency has been previously observed in FCL of short-chain COOH−$(CH_2)_{10}$−SH (MUA) monolayers when using lamination pressures up to 1.5 MPa and has been attributed to irreversible removal of *gauche* defects.[10a] The υ(Si−H) mode within the junction appears at 2084 cm^{-1} with a ≈40% area reduction compared to the freshly etched H−Si/Au sample, suggestive of monolayer−silicon interaction. Indeed, thiol bonding to the silicon surface has been shown in solution-based methods forming a robust Si−S linkage.[14c,58] The lack of SiO_2 vibrations in the 1000−1200 cm^{-1} region is consistent with a high-quality monolayer preventing oxidation of the silicon substrate.

While the temperature of DDT lamination is comparable to that of MHE (100 °C) and MHA (30−100 °C), the pressure required to laminate DDT was more than two times larger than the pressure needed to form MHE and MHA junctions. The modulus of elasticity obtained from close-packed aliphatic SAMs has been reported to be ≥20 GPa and exhibited a contact area dependence.[49] Separate nanotribology studies on confined *n*-alkanes in solution and perfluoroalkyl ether polymers reported a much lower force (2−10 MPa) needed for the structural transition from liquid state to solid state within the SAM.[56a,59] Temperature-induced softening of the aliphatic terminus can begin as low as 60 °C where *gauche* defects can be observed near the chain ends.[10a,34] Thus, it is possible that the loosely ordered DDT monolayers under 90 °C and 2.8 MPa undergo structural changes/deformation beyond the elastic limit, consistent with the decrease in the $\upsilon_{as}(CH_2)$ peak position observed in the IR, which may ultimately lead to SAM−Si adhesion.

Bonding of sulfur to silicon has been followed with X-ray absorption fine structure spectroscopy (NEXAFS) studies of C6-SH assembled on Si(111) by dissociative adsorption of the thiol to form Si−S and Si−H bonds on the surface, limiting molecular coverage and resulting in the formation of less-ordered monolayers.[60] The FCL junction is dominated by the self-assembly of the dithiol on gold prior to lamination, so we would not expect the same silicon adsorption constraints; however, these previous studies may shed light on the bonding process of the preformed monolayer with the Si−H surface during lamination. A higher temperature and pressure were needed during lamination of the DDT monolayer compared to the FCL conditions of MHE and MHA monolayers. This is not surprising considering the monolayer packing and end functionality are different with the DDT monolayer less ordered and less densely packed than MHA and MHE. Since there was no observation of Si−O or S−O species in the pb-RAIRS spectra of the Au−DDT−Si junction (Figure 2b), DDT is likely bonded by a C−S−Si linkage, not through sulfur oxidation species.

The water contact angle (≈70°) indicates a partial degree of hydrophobicity which would result in a minimal hydration layer of the exposed thiol. On the basis of the Young−Dupre eq 1, simple comparison of the CA_{H2O} from MHA (10°), MHE (90°), and DDT (70°) monolayers indicates the W_a would be in the following order: $W_{a(MHA)} > W_{a(DDT)} \geq W_{a(MHE)}$. The fact that DDT requires harsher lamination conditions than MHE to adhere to H−Si(111) indicates there is more to consider than surface free energy. These monolayers also differ in packing density/molecular orientation and, most notably, molecular functionality. Alkenes are known to bond to hydrogen-terminated silicon surfaces through an addition reaction involving hydrogen abstraction from the surface[61] that creates additional reactive sites facilitating a radical chain propagation mechanism for enhanced molecular attachment.[62] In the case of thiol−silicon bonding, this radical chain propagation is not applicable, and there arises the issue of excess hydrogen as the Si−H and S−H are cleaved to form a Si−S linkage. In solution-based reactions with hydrogen-terminated substrates, the hydrogen is thought to evolve as gas, but in this solid-state reaction, the diffusion and reactivity may be hindered at the molecule−silicon interface necessitating higher pressures and temperatures to achieve thiol lamination comparable to that of the alkene-terminated monolayer.

To further explore the value of this FCL approach, we have examined formation of nanoscale aromatic dithiol molecules tethered between silicon and gold electrodes. These molecules are particularly interesting from an electrical point of view because the conjugated π-electron system permits delocalization of electrons and, combined with ring rigidity, facilitates charge transport through the molecular layer. The terphenyl molecule of this study is a simple analogue of more complex molecules such as oligo phenylene ethynylenes which may have functional electrical behavior.[63] Previous studies have reported challenges in forming monolayers from aromatic dithiols for a variety of reasons, including the affinity between the aromatic ring and the metal surface leading to the molecules "lying down" on the surface, the formation of disulfide linkages leading to multilayer regions, and an oxidation of the sulfur atoms leading to sulfate species.[33,55c,64] We optimized experimental conditions for formation of 4−4′-*para*-terphenyldithiol (TPDT) to yield a single monolayer by tailoring the solution deposition time and sample rinsing following deposition, as detailed in the Materials and

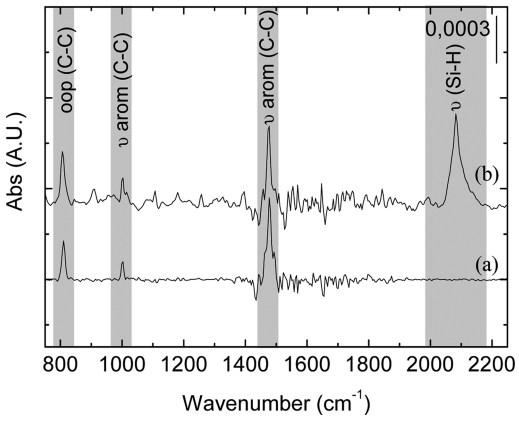

Figure 3. Reflection absorption spectrum of (a) free-standing TPDT−uSAu/PET and (b) pb-RAIRS spectrum of the FCL fabricated Si−TPDT−uSAu/PET junction.

Table 2. Vibrational Mode Assignments of TPDT[33b,a]

band position (cm^{-1})	mode assignment	Wilson notation	transition dipole moment
1475	ν(C−C) ring	19a	L
1100	ν(C−C) ring	15	M
1001	ν(C−C) ring	18a	L
808	δ(C−H)	10	N

[a] L: mode associated with a transition dipole moment oriented along the molecular axes. N: mode associated with a transition dipole moment perpendicular to the molecular axes. M: mode associated with a transition dipole moment oriented in the plane of the molecule and perpendicular to the molecular axes, see Scheme S2 (Supporting Information).

Methods section. The film thickness of 1.2 nm ± 0.2 nm derived from SE and the water contact angle of 72° ± 2° support the formation of a standing TPDT monolayer with the SH groups exposed to the air surface.[33a,65] The IR reflection absorption spectrum of free-standing TPDT on uSAu/PET (Figure 3a) exhibits peaks at 1479 and 1001 cm^{-1} assigned to υ(C═C) aromatic ring modes and a peak at 808 cm^{-1} assigned to the δ(C−H) ring mode, 19a, 18a, and 10, respectively, in the conventional Wilson notation for aromatic species, as presented in Table 2. The first two modes have transition dipole moments oriented along the long molecular axes (L), and the latter has a transition dipole moment perpendicular to the molecular plane (N), as depicted in the Supporting Information.[64a] The observation of both L and N related modes indicates that the TPDT molecules within the free-standing SAM are not oriented parallel to the metal surface. More detailed analysis of the molecular conformation for the IR data is presented in the Supporting Information. XPS analysis confirmed the presence of free SH groups and a surface coverage of 82%. (See Supporting Information.) Combined, these data suggest TPDT is present as a single monolayer with a decreased molecular density relative to the aliphatic monolayers.

After lamination at 90 °C and 2.8 MPa (Figure 3b), the peaks observed in the spectrum obtained from the FCL junction show small increases in absorbance intensity and broadening of all of the observed peaks to suggest increased monolayer inhomogeneity. The presence of C−C aromatic ring modes indicates the aromaticity of TPDT is not compromised upon lamination despite the affinity of π-conjugated structures to bind to Si.[66] Thus, it is likely that the monolayer anchors to Si through the thiol group, similar to DDT and consistent with previous studies of benzenethiol on Si(001).[67] In this TPDT sandwich structure, the υ(Si−H) mode appears broader at 2084 cm^{-1}. Interestingly, the integrated intensity of the Si−H mode is quite large compared with the other FCL molecular junctions in this study. Previous studies of aromatic thiol molecules attached to silicon attributed the presence of large Si−H peaks to the hydrogen cleavage from either dehydrogenation of the thiol group or H that cannot leave the surface as H_2.[67] FCL of TPDT takes place under the same conditions as DDT consistent with the similar surface free energy and suggests the more aggressive lamination conditions needed for thiol-terminated monolayers are related to the Si−S interaction rather than pressure-induced molecular reorientation.

The structural characterization performed by pb-RAIRS demonstrates that monolayers confined between the gold and silicon substrates maintain the molecular conformation of the free-standing monolayer. The short-chain ω-functionalized alkylthiols undergo structural changes to slightly improve the aliphatic backbone orientation. Lamination conditions differ for each molecular junction to maintain molecular quality and ensure adhesion with H−Si(111). This means that slightly different temperatures and pressures were needed to form reliable molecular junctions with these conditions dictated by the end functional group that is interacting with the Si−H surface. In the case of acid-terminated monolayers, we hypothesize that bonding is facilitated by a hydration layer on the hydrophilic monolayer leading to junction formation. Alkene-terminated monolayers are lacking this hydration layer, necessitating slightly higher temperature conditions which likely contribute to conformational changes making the terminal C═C more accessible to interaction with the Si−H. Both aromatic and aliphatic monolayers terminated in thiol functional groups formed molecular junctions under similar FCL conditions. These conditions included elevated temperature and pressure and are likely due to a larger energy barrier for attachment due to the lack of a hydration layer and the presence of excess hydrogen which pollutes the interface.

Electrical Properties. Because transport within a junction is a very sensitive indication of the molecular junction quality, we measured the current−voltage (I−V) characteristics of the nanoscale molecular architectures fabricated with FCL. In addition, there is a large interest in harnessing organic molecules for electronic purposes. Figure 4a shows current−voltage (I−V) data obtained from Au−monolayer−Si junctions of MHA, MHE, DDT, and TPDT with an area of 1.76×10^{-4} cm^2 as well as a metal−Si control. The highly doped n-type silicon substrate was grounded, and the bias was applied to the top metal electrode. These data are average I−V curves obtained from the individual molecular junctions (≈90% electric yield). The magnitude of measured current exhibited for the molecular junctions is attenuated compared to the control. The current within a heavily doped silicon−metal junction is very sensitive to the presence of an insulator, and the observation of this attenuation indicates the molecular layer is behaving as an ultrathin dielectric. The current densities measured for these devices are about an order of magnitude higher than previously reported Si−molecule−Hg devices;[68] however, they are the same order of magnitude as previous large-area devices made with nanotransfer printing techniques.[24b,69] Unlike metal-based molecular junctions, where there is clear molecular length dependence from tunneling

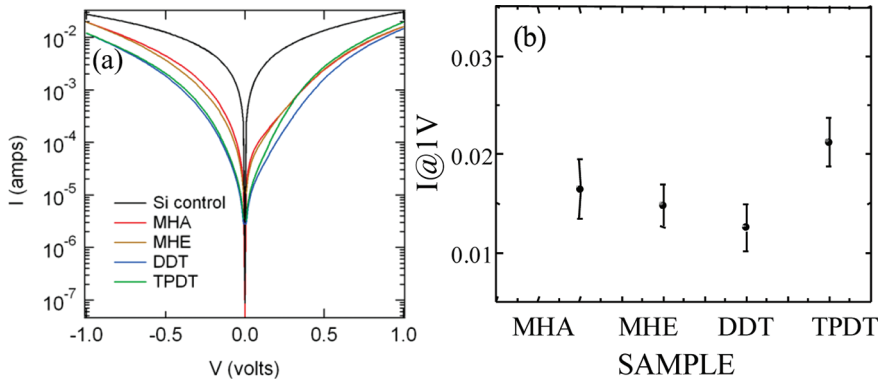

Figure 4. (a) Logarithmic current−voltage data obtained from MHA, MHE, DDT, and TPDT within the FCL molecular junctions and a control metal−Si reference. (b) Current within the FCL structures obtained at 1 V forward bias.

observed in the magnitude of measured current, silicon-based molecular electronic junctions are more complicated. Depending on the doping of the semiconductor and the junction formation, transport is often a complex interplay of the molecule and semiconductor and can even be dominated by the top metal and the method of junction fabrication.[68b,70]

MHA and MHE are molecular junctions with similar current consisting of a hexadecane chain and differ in the headgroup which reacts with silicon. The shorter-chain aliphatic molecular junctions, DDT, have smaller than expected currents. The TPDT represents an aromatic system of length close to DDT. At reverse bias and low forward bias, the current of these two dithiols is similar. At high forward bias, where the tunneling regime dominates, TPDT shows higher current than the saturated alkylthiol monolayers (see Figure 4b). In particular, when comparing the currents for TPDT and DDT, which have similar molecular length and similar bonding to the electrodes, the effect of the π-conjugation is clearly observed in the higher bias regime. For saturated alkyl junctions, the dominant charge transport mechanism is described as direct tunneling.[15c,71] While charge transport through π-conjugated molecules is more complex and less well understood,[72] the conductivity is expected to be one to ten times higher than aliphatic chains due to extended π-electronic orbitals which span the molecular length.[73]

In the low forward bias (0−0.2 V) regime and the reverse bias regime, the current in the MHA and MHE junctions is similar, and the TPDT and DDT junctions exhibit very similar current values (see Supporting Information).[74] This is consistent with previous studies where charge transport was dominated by the large surface dipole layer induced by the monolayer and the space charge region of the semiconductor.[68c] For such junctions, the current in low forward bias is predicted to be limited by transport over the Schottky barrier in silicon and not expected to exhibit any alkyl dependence.[27b] The reverse bias characteristics suggest that the Schottky barrier is higher for Si−S than for Si−C or Si−OOC. The expected better mobility of the conjugated wire (TPDT) compensates for the more blocking Schottky barrier only at ≈+0.3 V. The Supporting Information section contains a more detailed discussion of the Si−molecule−metal electrical results.

Metal−molecule−metal junctions have exhibited current densities dependent on the molecular length and show distinctly different resistance for molecules with two chemisorbed contacts compared to one chemisorbed/physisorbed contact.[75] In our work, the nature of this second contact could affect the electrical properties in a variety of ways since the second electrode is a semiconductor. First, we assume that all of the molecules are attached to the Au substrate since self-assembly occurs on this surface and the substrates are cleaned to remove excess material not bonded to the Au. This provides one chemisorbed contact and leaves the second functional group to bond with silicon during the FCL process. From a mechanical perspective, this bonding of the second functional group with the silicon serves to adhere the gold electrode, creating a uniform nanoelectronic device thickness. Typically, variations in the device thickness manifest in variations in the electrical conductivity due to thickness-dependent tunneling. We expect electrode spacing variations to be minimal in our FCL-fabricated devices since both substrates are quite smooth, ultrasmooth gold, and H−Si, and the Au surface is on a flexible polymer backing that allows conformal adhesion to the silicon substrate.

The molecule−silicon bonding reaction can also affect the properties of the silicon by creating an interfacial dipole and/or inducing charge transfer between the silicon and the molecular layer.[5b,23c,23d,76] This effect is much larger than the geometric considerations described above and can shift properties by several meV. The slight differences observed for MHA and MHE (Figure 4) are consistent with reported dipole differences of molecules bonded through a Si−O linkage relative to the Si−C and Si−S interface.[76a] Previous mercury junction reports observed a lower barrier height for Si−O−C molecular junctions than Si−C junctions,[68b] consistent with our MHA conductivity observations. The third effect bonding can have is to alter the electronic properties of the silicon interface. Silicon is known to have defect states within the bandgap, sometimes arising from dangling bonds or differences in hydrogen termination, which can be responsible for Fermi level pinning or defect-mediated trap states.[77] Bonding of molecules to the silicon surface can remove these defect states, as well as remove the propensity of silicon to oxidize.[78] Finally, from an electronics standpoint, bonding to silicon presents a more facile route to charge transfer as the electronic wave function of the silicon and molecule overlap to increase the transfer probability.[79] Previous work has shown that the bonding of molecules to silicon creates an induced density of states (IDIS) at the interface due to the covalent attachment of organics to the silicon surface[79] which effectively dominates charge transport across these surfaces.[80] In all likelihood, electronic transport across metal−molecule−semiconductor systems contains contributions from a number of these effects (dipole, charge transfer, defect states, IDIS) with the relative weight of each factor determined by the molecular layer and

semiconductor doping.[14c,74,68a,81] Thorough temperature-dependent $I-V$ measurements are underway to enable a more complete interpretation of the charge transport mechanism through these FCL junctions.[82]

CONCLUSIONS

The flip-chip lamination technique is a crucial advancement in the fabrication of nanoscale molecular architectures as a variety of organic molecules can be chemically bonded to both electrodes while maintaining the structural and electrical properties of the molecular layer. We report the formation of metal−monolayer−silicon junctions made with alkyl or aromatic monolayers chemically bonded to Au via thiol chemistry and bound to silicon via either Si−C, Si−O−C, or Si−S bonds. Thorough characterization of the molecular structure before lamination and after the monolayer was encased within the electrodes indicates the molecular layer remains intact with minimal changes in the backbone structure and changes in the functionalities due to bonding with the silicon surface. In all cases, the molecular conformation is preserved or slightly rearranged upon adhesion to H−Si(111). The externally applied pressure and temperature must be varied in accordance with the SAM surface free energy, monolayer conformation, ambient humidity, and molecular functionality to ensure effective chemical bonding between the monolayers and the H−Si(111) surface. Both pb-RAIRS and $I-V$ measurements confirm the presence of the organic monolayer between electrodes demonstrating FCL as a route for systematic screening of molecular junctions between the two bulk materials with a gentle contacting method. Electrical differences were observed between π-conjugated and alkyl backbones attributed to the extended π-delocalization where minimal variations are identified due to the chemical nature of Si-atom linkage. Because FCL relies on the formation of monolayers on the more amenable gold surface first, we are able to examine a range of molecular layers on silicon of very high quality that are not accessible by directly assembling the molecules on silicon. This opens many avenues for silicon-based molecular electronics as further physical and chemical metrology are accessible to identify the underlying molecule−electrode properties to harness the potential of organic molecules for electronic, magnetic, optoelectronic, chemical, biological, and medical applications.

ASSOCIATED CONTENT

Supporting Information. Additional experimental data of XPS and electrical measurements. This material is available free of charge via the Internet at http://pubs.acs.org.

AUTHOR INFORMATION

Corresponding Author

*E-mail: christina.hacker@nist.gov.

Present Addresses

[†]Institut de Ciencia de Materials de Barcelona (ICMAB-CSIC), Campus de la UAB, Barcelona, Spain 08193.

[‡]Mary Baldwin College, Staunton, VA 24402.

ACKNOWLEDGMENT

The authors would like to thank Prof. E.D. Williams for helpful discussions. Research performed in part at the nanofabrication facility within the NIST Center for Nanoscale Science and Technology.

REFERENCES

(1) (a) Aviram, A. Molecules for Memory, Logic, and Amplification. *J. Am. Chem. Soc.* **1988**, *110* (17), 5687–5692. (b) Lu, W.; Lieber, C. M. Nanoelectronics from the bottom up. *Nat. Mater.* **2007**, *6* (11), 841–850. (c) Tour, J. M.; Kozaki, M.; Seminario, J. M. Molecular scale electronics: A synthetic/computational approach to digital computing. *J. Am. Chem. Soc.* **1998**, *120* (33), 8486–8493.

(2) (a) Har-Lavan, R.; Ron, I.; Thieblemont, F.; Cahen, D. Toward metal-organic insulator-semiconductor solar cells, based on molecular monolayer self-assembly on n-Si. *Appl. Phys. Lett.* **2009**, *94* (4), 043308. (b) Schmidt-Mende, L.; Fechtenkotter, A.; Mullen, K.; Moons, E.; Friend, R. H.; MacKenzie, J. D. Self-organized discotic liquid crystals for high-efficiency organic photovoltaics. *Science* **2001**, *293* (5532), 1119–1122.

(3) (a) Kovalenko, M. V.; Scheele, M.; Talapin, D. V. Colloidal Nanocrystals with Molecular Metal Chalcogenide Surface Ligands. *Science* **2009**, *324* (5933), 1417–1420. (b) Torsi, L.; Dodabalapur, A.; Rothberg, L. J.; Fung, A. W. P.; Katz, H. E. Intrinsic transport properties and performance limits of organic field-effect transistors. *Science* **1996**, *272* (5267), 1462–1464.

(4) (a) Cattani-Scholz, A.; Pedone, D.; Dubey, M.; Neppl, S.; Nickel, B.; Feulner, P.; Schwartz, J.; Abstreiter, G.; Tornow, M. Organophosphonate-based PNA-functionalization of silicon nanowires for label-free DNA detection. *ACS Nano* **2008**, *2* (8), 1653–1660. (b) Pike, A. R.; Lie, L. H.; Eagling, R. A.; Ryder, L. C.; Patole, S. N.; Connolly, B. A.; Horrocks, B. R.; Houlton, A. DNA on silicon devices: On-chip synthesis, hybridization, and charge transfer. *Angew. Chem., Int. Ed.* **2002**, *41* (4), 615–617.

(5) (a) Stewart, M. P.; Maya, F.; Kosynkin, D. V.; Dirk, S. M.; Stapleton, J. J.; McGuiness, C. L.; Allara, D. L.; Tour, J. M. Direct covalent grafting of conjugated molecules onto Si, GaAs, and Pd surfaces from aryidiazonium salts. *J. Am. Chem. Soc.* **2004**, *126* (1), 370–378. (b) Aswal, D. K.; Lenfant, S.; Guerin, D.; Yakhmi, J. V.; Vuillaume, D. Self assembled monolayers on silicon for molecular electronics. *Anal. Chim. Acta* **2006**, *568* (1−2), 84–108. (c) Vuillaume, D.; Boulas, C.; Collet, J.; Allan, G.; Delerue, C. Electronic structure of a heterostructure of an alkylsiloxane self-assembled monolayer on silicon. *Phys. Rev. B* **1998**, *58* (24), 16491–16498. (d) Vilan, A.; Yaffe, O.; Biller, A.; Salomon, A.; Kahn, A.; Cahen, D. Molecules on Si: Electronics with Chemistry. *Adv. Mater.* **2010**, *22* (2), 140–159.

(6) Rakshit, T.; Liang, G. C.; Ghosh, A. W.; Datta, S. Silicon-based molecular electronics. *Nano Lett.* **2004**, *4* (10), 1803–1807.

(7) McCreery, R. L.; Bergren, A. J. Progress with Molecular Electronic Junctions: Meeting Experimental Challenges in Design and Fabrication. *Adv. Mater.* **2009**, *21* (43), 4303–4322.

(8) McCreery, R. L. Molecular electronic junctions. *Chem. Mater.* **2004**, *16* (23), 4477–4496.

(9) Ranganathan, S. S., I.; Anariba, F.; McCreery, R. L. Covalently Bonded Organic Monolayers on a Carbon Substrate: A New Paradigm for Molecular Electronics. *Nano Lett.* **2001**, *1* (9), 491–494.

(10) (a) Coll, M.; Miller, L. H.; Richter, L. J.; Hines, D. R.; Jurchescu, O. D.; Gergel-Hackett, N.; Richter, C. A.; Hacker, C. A. Formation of Silicon-Based Molecular Electronic Structures Using Flip-Chip Lamination. *J. Am. Chem. Soc.* **2009**, *131* (34), 12451–12457. (b) Wagner, P.; Hegner, M.; Guntherodt, H. J.; Semenza, G. Formation and in-Situ Modification of Monolayers Chemisorbed on Ultraflat Template-Stripped Gold Surfaces. *Langmuir* **1995**, *11* (10), 3867–3875. (c) Weiss, E. A.; Chiechi, R. C.; Kaufman, G. K.; Kriebel, J. K.; Li, Z. F.; Duati, M.; Rampi, M. A.; Whitesides, G. M. Influence of defects on the electrical characteristics of mercury-drop junctions: Self-assembled monolayers of n-alkanethiolates on rough and smooth silver. *J. Am. Chem. Soc.* **2007**, *129* (14), 4336–4349.

(11) Mahapatro, A. K.; Scott, A.; Manning, A.; Janes, D. B. Gold surface with sub-nm roughness realized by evaporation on a molecular adhesion monolayer. *Appl. Phys. Lett.* **2006**, *88* (15), 151917.

(12) (a) Dumas, P.; Chabal, Y. J.; Jakob, P. Morphology of Hydrogen-Terminated Si(111) and Si(100) Surfaces Upon Etching in Hf and Buffered-Hf Solutions. *Surf. Sci.* **1992**, *269*, 867–878. (b) Higashi, G. S.; Becker, R. S.; Chabal, Y. J.; Becker, A. J. Comparison of Si(111) Surfaces Prepared Using Aqueous-Solutions of Nh4f Versus Hf. *Appl. Phys. Lett.* **1991**, *58* (15), 1656–1658.

(13) (a) Li, X. L.; He, J.; Hihath, J.; Xu, B. Q.; Lindsay, S. M.; Tao, N. J. Conductance of single alkanedithiols: Conduction mechanism and effect of molecule-electrode contacts. *J. Am. Chem. Soc.* **2006**, *128* (6), 2135–2141. (b) Tao, N. J. Electron transport in molecular junctions. *Nat. Nanotechnol.* **2006**, *1* (3), 173–181. (c) Venkataraman, L.; Klare, J. E.; Tam, I. W.; Nuckolls, C.; Hybertsen, M. S.; Steigerwald, M. L. Single-molecule circuits with well-defined molecular conductance. *Nano Lett.* **2006**, *6* (3), 458–462. (d) Selzer, Y.; Salomon, A.; Cahen, D. The importance of chemical bonding to the contact for tunneling through alkyl chains. *J. Phys. Chem. B* **2002**, *106* (40), 10432–10439.

(14) (a) Quek, S. Y.; Kamenetska, M.; Steigerwald, M. L.; Choi, H. J.; Louie, S. G.; Hybertsen, M. S.; Neaton, J. B.; Venkataraman, L. Mechanically controlled binary conductance switching of a single-molecule junction. *Nat. Nanotechnol.* **2009**, *4* (4), 230–234. (b) Venkataraman, L.; Park, Y. S.; Whalley, A. C.; Nuckolls, C.; Hybertsen, M. S.; Steigerwald, M. L. Electronics and chemistry: Varying single-molecule junction conductance using chemical substituents. *Nano Lett.* **2007**, *7* (2), 502–506. (c) Hacker, C. A. Modifying electron transfer at the silicon-molecule interfance using atomic tethers. *Solid-State Electron.* **2010**, *54* (12), 1657–1664. (d) Nitzan, A.; Galperin, M.; Ingold, G. L.; Grabert, H. On the electrostatic potential profile in biased molecular wires. *J. Chem. Phys.* **2002**, *117* (23), 10837–10841. (e) Rissner, F.; Egger, D. A.; Romaner, L.; Heimel, G.; Zojer, E., The Electronic Structure of Mixed Self-Assembled Monolayers. *ACS Nano 4* (11), 6735-6746; (f) Gergel-Hackett, N.; Aguilar, I.; Richter, C. A. Engineering the Electron Transport of Silicon-Based Molecular Electronic Devices via Molecular Dipoles. *J. Phys. Chem. C* **2010**, *114* (49), 21708–21714.

(15) (a) Venkataraman, L.; Klare, J. E.; Nuckolls, C.; Hybertsen, M. S.; Steigerwald, M. L. Dependence of single-molecule junction conductance on molecular conformation. *Nature* **2006**, *442* (7105), 904–907. (b) Beebe, J. M.; Kim, B.; Frisbie, C. D.; Kushmerick, J. G. Measuring relative barrier heights in molecular electronic junctions with transition voltage spectroscopy. *ACS Nano* **2008**, *2* (5), 827–832. (c) Choi, S. H.; Kim, B.; Frisbie, C. D. Electrical resistance of long conjugated molecular wires. *Science* **2008**, *320* (5882), 1482–1486.

(16) Segev, L.; Salomon, A.; Natan, A.; Cahen, D.; Kronik, L.; Amy, F.; Chan, C. K.; Kahn, A. Electronic structure of Si(111)-bound alkyl monolayers: Theory and experiment. *Phys. Rev. B* **2006**, *74* (16), 165323.

(17) (a) McGuiness, C. L.; Blasini, D.; Masejewski, J. P.; Uppili, S.; Cabarcos, O. M.; Smilgies, D.; Allara, D. L. Molecular Self-Assembly at Bare Semiconductor Surfaces: Characterization of a Homologous Series of n-Alkanethiolate Monolayers on GaAs(001). *ACS Nano* **2007**, *1* (1), 30–49. (b) McGuiness, C. L.; Shaporenko, A.; Zharnikov, M.; Walker, A. V.; Allara, D. L. Molecular Self-Assembly at Bare Semiconductor Surfaces: Investigation of the Chemical and Electronic Properties of the Alkanethiolateâ'GaAs(001) Interface. *J. Phys. Chem. C* **2007**, *111* (11), 4226–4234.

(18) Ishizaki, T.; Saito, N.; SunHyung, L.; Ishida, K.; Takai, O. Study of Alkyl Organic Monolayers with Different Molecular Chain Lengths Directly Attached to Silicon. *Langmuir* **2006**, *22* (24), 9962–9966.

(19) Schreiber, F. Structure and growth of self-assembling monolayers. *Prog. Surf. Sci.* **2000**, *65* (5−8), 151–256.

(20) (a) Maldonado, S.; Plass, K. E.; Knapp, D.; Lewis, N. S. Electrical Properties of Junctions between Hg and Si(111) Surfaces Functionalized with Short-Chain Alkyls. *J. Phys. Chem. C* **2007**, *111* (48), 17690–17699. (b) Hacker, C. A.; Richter, C. A.; Gergel-Hackett, N.; Richter, L. J. Origin of differing reactivities of aliphatic chains on H-Si(111) and oxide surfaces with metal. *J. Phys. Chem. C* **2007**, *111* (26), 9384–9392. (c) Hacker, C. A.; Anderson, K. A.; Richter, L. J.; Richter, C. A. Comparison of Si-O-C interfacial bonding of alcohols and aldehydes on Si(111) formed from dilute solution with ultraviolet irradiation. *Langmuir* **2005**, *21* (3), 882–889. (d) Richter, C. A.; Hacker, C. A.; Richter, L. J.; Vogel, E. M. Molecular devices formed by direct monolayer attachment to silicon. *Solid-State Electron.* **2004**, *48* (10−11), 1747–1752. (e) Hurley, P. T.; Ribbe, A. E.; Buriak, J. M. Nanopatterning of alkynes on hydrogen-terminated silicon surfaces by scanning probe-induced cathodic electrografting. *J. Am. Chem. Soc.* **2003**, *125* (37), 11334–11339. (f) Wacaser, B. A.; Maughan, M. J.; Mowat, I. A.; Niederhauser, T. L.; Linford, M. R.; Davis, R. C. Chemomechanical surface patterning and functionalization of silicon surfaces using an atomic force microscope. *Appl. Phys. Lett.* **2003**, *82* (5), 808–810.

(21) Buriak, J. M. Organometallic chemistry on silicon and germanium surfaces. *Chem. Rev.* **2002**, *102* (5), 1271–1308.

(22) (a) Miramond, C.; Vuillaume, D. 1-octadecene monolayers on Si(111) hydrogen-terminated surfaces: Effect of substrate doping. *J. Appl. Phys.* **2004**, *96* (3), 1529–1536. (b) Richter, C. A.; Hacker, C. A.; Richter, L. J. Electrical and spectroscopic characterization of metal/monolayer/Si devices. *J. Phys. Chem. B* **2005**, *109* (46), 21836–21841.

(23) (a) Allongue, P.; de Villeneuve, C. H.; Cherouvrier, G.; Cortes, R.; Bernard, M. C. Phenyl layers on H-Si(111) by electrochemical reduction of diazonium salts: monolayer versus multilayer formation. *J. Electroanal. Chem.* **2003**, *550*, 161–174. (b) Scott, A.; Hacker, C. A.; Janes, D. B. In situ structural characterization of metal-molecule-silicon junctions using backside infrared spectroscopy. *J. Phys. Chem. C* **2008**, *112* (36), 14021–14026. (c) He, T.; Ding, H. J.; Peor, N.; Lu, M.; Corley, D. A.; Chen, B.; Ofir, Y.; Gao, Y. L.; Yitzchaik, S.; Tour, J. M. Silicon/molecule interfacial electronic modifications. *J. Am. Chem. Soc.* **2008**, *130* (5), 1699–1710. (d) Hunger, R.; Jaegermann, W.; Merson, A.; Shapira, Y.; Pettenkofer, C.; Rappich, J. Electronic structure of methoxy-, bromo-, and nitrobenzene grafted onto Si(111). *J. Phys. Chem. B* **2006**, *110* (31), 15432–15441. (e) Anariba, F.; DuVall, S. H.; McCreery, R. L. Mono- and multilayer formation by diazonium reduction on carbon surfaces monitored with atomic force microscopy "scratching". *Anal. Chem.* **2003**, *75* (15), 3837–3844.

(24) (a) Haick, H.; Cahen, D. Contacting organic molecules by soft methods: Towards molecule-based electronic devices. *Acc. Chem. Res.* **2008**, *41* (3), 359–366. (b) Loo, Y. L.; Lang, D. V.; Rogers, J. A.; Hsu, J. W. P. Electrical contacts to molecular layers by nanotransfer printing. *Nano Lett.* **2003**, *3* (7), 913–917. (c) Hacker, C. A.; Coll, M.; Richter, C. A. Metrology of Molecular Devices made by Flip Chip Lamination. *Electrochem. Soc. Trans.* **2010**, *28*, 549–562.

(25) (a) Jung, D. R.; Czanderna, A. W. Chemical and Physical Interactions at Metal Self-Assembled Organic Monolayer Interfaces. *Crit. Rev. Solid State Mater. Sci.* **1994**, *19* (1), 1–54. (b) Stewart, D. R.; Ohlberg, D. A. A.; Beck, P. A.; Chen, Y.; Williams, R. S.; Jeppesen, J. O.; Nielsen, K. A.; Stoddart, J. F. Molecule-independent electrical switching in Pt/organic monolayer/Ti devices. *Nano Lett.* **2004**, *4* (1), 133–136. (c) Tai, Y.; Shaporenko, A.; Eck, W.; Grunze, M.; Zharnikov, M. Abrupt change in the structure of self-assembled monolayers upon metal evaporation. *Appl. Phys. Lett.* **2004**, *85* (25), 6257–6259. (d) Walker, A. V.; Tighe, T. B.; Cabarcos, O. M.; Reinard, M. D.; Haynie, B. C.; Uppili, S.; Winograd, N.; Allara, D. L. The dynamics of noble metal atom penetration through methoxy-terminated alkanethiolate monolayers. *J. Am. Chem. Soc.* **2004**, *126* (12), 3954–3963.

(26) (a) de Boer, B.; Frank, M. M.; Chabal, Y. J.; Jiang, W. R.; Garfunkel, E.; Bao, Z. Metallic contact formation for molecular electronics: interactions between vapor-deposited metals and self-assembled monolayers of conjugated mono- and dithiols. *Langmuir* **2004**, *20* (5), 1539–1542. (b) Hooper, A.; Fisher, G. L.; Konstadinidis, K.; Jung, D.; Nguyen, H.; Opila, R.; Collins, R. W.; Winograd, N.; Allara, D. L. Chemical effects of methyl and methyl ester groups on the nucleation and growth of vapor-deposited aluminum films. *J. Am. Chem. Soc.* **1999**, *121* (35), 8052–8064. (c) Walker, A. V.; Tighe, T. B.; Stapleton, J.; Haynie, B. C.; Upilli, S.; Allara, D. L.; Winograd, N. Interaction of vapor-deposited Ti and Au with molecular wires. *Appl. Phys. Lett.* **2004**, *84* (20), 4008–4010.

(27) (a) Liu, Y. J.; Yu, H. Z. Molecular passivation of mercury-silicon (p-type) diode junctions: Alkylation, oxidation, and alkylsilation. *J. Phys.*

Chem. B **2003**, *107* (31), 7803–7811. (b) Salomon, A.; Bocking, T.; Gooding, J. J.; Cahen, D. How Important is the Interfacial Chemical Bond for Electron Transport through Alkyl Chain Monolayers. *Nano Lett.* **2006**, *6* (12), 2873–2876.

(28) Haick, H.; Niitsoo, O.; Ghabboun, J.; Cahen, D. Electrical contacts to organic molecular films by metal evaporation: Effect of contacting details. *J. Phys. Chem. C* **2007**, *111* (5), 2318–2329.

(29) (a) Vilan, A.; Ghabboun, J.; Cahen, D. Molecule-metal polarization at rectifying GaAs interfaces. *J. Phys. Chem. B* **2003**, *107* (26), 6360–6376. (b) Stein, N.; Korobko, R.; Yaffe, O.; Lavan, R. H.; Shpaisman, H.; Tirosh, E.; Vilan, A.; Cahen, D. Nondestructive Contact Deposition for Molecular Electronics: Si-Alkyl//Au Junctions. *J. Phys. Chem. C* **2010**, *114* (29), 12769–12776. (c) Shimizu, K. T.; Fabbri, J. D.; Jelincic, J. J.; Melosh, N. A. Soft deposition of large-area metal contacts for molecular electronics. *Adv. Mater.* **2006**, *18* (12), 1499–1504. (d) Stein, N.; Korobko, R.; Yaffe, O.; Lavan, R. H.; Shpaisman, H.; Tirosh, E.; Vilan, A.; Cahen, D. Nondestructive Contact Deposition for Molecular Electronics: Si-Alkyl//Au Junctions. *J. Phys. Chem. C* **2010**, *114* (29), 12769–12776.

(30) Coll, M.; Goetz, K. P.; Conrad, B. R.; Hacker, C. A.; Gundlach, D. J.; Richter, C. A.; Jurchescu, O. D. Flip chip lamination to electrically contact organic single crystals on flexible substrates. *Appl. Phys. Lett.* **2011**, *98*, 16.

(31) Bain, C. D.; Troughton, E. B.; Tao, Y. T.; Evall, J.; Whitesides, G. M.; Nuzzo, R. G. Formation of Monolayer Films by the Spontaneous Assembly of Organic Thiols from Solution onto Gold. *J. Am. Chem. Soc.* **1989**, *111* (1), 321–335.

(32) Richter, C. A.; Hacker, C. A.; Richter, L. J.; Kirillov, O. A.; Suehle, J. S.; Vogel, E. M. Interface characterization of molecular-monolayer/SiO2 based molecular junctions. *Solid-State Electron.* **2006**, *50* (6), 1088–1096.

(33) (a) de Boer, B.; Meng, H.; Perepichka, D. F.; Zheng, J.; Frank, M. M.; Chabal, Y. J.; Bao, Z. N. Synthesis and characterization of conjugated mono- and dithiol oligomers and characterization of their self-assembled monolayers. *Langmuir* **2003**, *19* (10), 4272–4284. (b) Weckenmann, U.; Mittler, S.; Naumann, K.; Fischer, R. A. Ordered self-assembled monolayers of 4,4′-biphenyldithiol on polycrystalline silver: Suppression of multilayer formation by addition of tri-n-butylphosphine. *Langmuir* **2002**, *18* (14), 5479–5486.

(34) Coll, M.; Richter, C. A.; Hacker, C. A. Thermal stability of confined flip-chip laminated omega-functionalized monolayers. *J. Vac. Sci. Technol. B* **2009**, *27* (6), 2826–2831.

(35) Snyder, R. G.; Strauss, H. L.; Elliger, C. A. C-H Stretching Modes and the Structure of Normal-Alkyl Chains 0.1. Long, Disordered Chains. *J. Phys. Chem.* **1982**, *86* (26), 5145–5150.

(36) Peanasky, J. S.; McCarley, R. L. Surface-confined monomers on electrode surfaces. 4. Electrochemical and spectroscopic characterization of undec-10-ene-1-thiol self-assembled monolayers on Au. *Langmuir* **1998**, *14* (1), 113–123.

(37) Greenler, R. G. Infrared Study of Adsorbed Molecules on Metal Surfaces by Reflection Techniques. *J. Chem. Phys.* **1966**, *44* (1), 310–315.

(38) Higashi, G. S.; Chabal, Y. J.; Trucks, G. W.; Raghavachari, K. Ideal Hydrogen Termination of the Si-(111) Surface. *Appl. Phys. Lett.* **1990**, *56* (7), 656–658.

(39) Amy, S. R.; Michalak, D. J.; Chabal, Y. J.; Wielunski, L.; Hurley, P. T.; Lewis, N. S. Investigation of the reactions during alkylation of chlorine-terminated silicon (111) surfaces. *J. Phys. Chem. C* **2007**, *111* (35), 13053–13061.

(40) Michalak, D. J.; Rivillon, S.; Chabal, Y. J.; Esteve, A.; Lewis, N. S. Infrared spectroscopic investigation of the reaction of hydrogen-terminated, (111)-oriented, silicon surfaces with liquid methanol. *J. Phys. Chem. B* **2006**, *110* (41), 20426–20434.

(41) (a) Linford, M. R.; Fenter, P.; Eisenberger, P. M.; Chidsey, C. E. D. Alkyl Monolayers on Silicon Prepared from 1-Alkenes and Hydrogen-Terminated Silicon. *J. Am. Chem. Soc.* **1995**, *117* (11), 3145–3155. (b) Webb, L. J.; Rivillon, S.; Michalak, D. J.; Chabal, Y. J.; Lewis, N. S. Transmission infrared spectroscopy of methyl- and ethyl-terminated silicon(111) surfaces. *J. Phys. Chem. B* **2006**, *110* (14), 7349–7356.

(42) (a) Sieval, A. B.; van den Hout, B.; Zuilhof, H.; Sudholter, E. J. R. Molecular modeling of alkyl monolayers on the Si(111) surface. *Langmuir* **2000**, *16* (7), 2987–2990. (b) Weldon, M. K.; Marsico, V. E.; Chabal, Y. J.; Hamann, D. R.; Christman, S. B.; Chaban, E. E. Infrared spectroscopy as a probe of fundamental processes in microelectronics: Silicon wafer cleaning and bonding. *Surf. Sci.* **1996**, *368*, 163–178.

(43) Liu, Y. J.; Wang, Z. G.; Suo, Y. R. Theoretical study on the mechanism for the addition reaction of SiH3 with propylene and acetic acid. *J. Phys. Chem. A* **2006**, *110* (45), 12439–12442.

(44) (a) Asanuma, H.; Lopinski, G. P.; Yu, H. Z. Kinetic control of the photochemical reactivity of hydrogen-terminated silicon with bifunctional molecules. *Langmuir* **2005**, *21* (11), 5013–5018. (b) Boukherroub, R.; Wayner, D. D. M. Controlled Functiontalization and Multistep Chemical Manipulation of Covalently Modified Si (111) Surfaces. *J. Am. Chem. Soc.* **1999**, *121* (49), 11513–11515.

(45) Carpick, R. W.; Salmeron, M. Scratching the surface: Fundamental investigations of tribology with atomic force microscopy. *Chem. Rev.* **1997**, *97* (4), 1163–1194.

(46) Nuzzo, R. G.; Dubois, L. H.; Allara, D. L. Fundamental-Studies of Microscopic Wetting on Organic-Surfaces 0.1. Formation and Structural Characterization of a Self-Consistent Series of Polyfunctional Organic Monolayers. *J. Am. Chem. Soc.* **1990**, *112* (2), 558–569.

(47) Arnold, R.; Azzam, W.; Terfort, A.; Woll, C. Preparation, Modification, and Crystallinity of Aliphatic and Aromatic Carboxylic Acid Terminated Self-Assembled Monolayers. *Langmuir* **2002**, *18* (10), 3980–3992.

(48) (a) Bhushan, B.; Liu, H. W. Nanotribological properties and mechanisms of alkylthiol and biphenyl thiol self-assembled monolayers studied by AFM. *Phys. Rev. B* **2001**, *6324* (24), 245412. (b) Schrader, M. E. Young-Dupre Revisited. *Langmuir* **1995**, *11* (9), 3585–3589. (c) Green, J.-B. D.; McDermott, M. T.; Porter, M. D.; Siperko, L. M. Nanometer-Scale Mapping of Chemically Distinct Domains at Well-Defined Organic Interfaces Using Frictional Force Microscopy. *J. Phys. Chem.* **1995**, *99* (27), 10960–10965.

(49) Berg, O.; Klenerman, D. Vibrational spectroscopy of mechanically compressed monolayers. *J. Am. Chem. Soc.* **2003**, *125* (18), 5493–5500.

(50) Cicero, R. L.; Chidsey, C. E. D.; Lopinski, G. P.; Wayner, D. D. M.; Wolkow, R. A. Olefin additions on H-Si(111): Evidence for a surface chain reaction initiated at isolated dangling bonds. *Langmuir* **2002**, *18* (2), 305–307.

(51) Szori, M.; Jedlovszky, P.; Roeselova, M. Water adsorption on hydrophilic and hydrophobic self-assembled monolayers as proxies for atmospheric surfaces. A grand canonical Monte Carlo simulation study. *Phys. Chem. Chem. Phys.* **2010**, *12* (18), 4604–4616.

(52) (a) Xiao, X. D.; Qian, L. M. Investigation of humidity-dependent capillary force. *Langmuir* **2000**, *16* (21), 8153–8158. (b) Qian, L. M.; Tian, F.; Xiao, X. D. Tribological properties of self-assembled monolayers and their substrates under various humid environments. *Tribol. Lett.* **2003**, *15* (3), 169–176.

(53) Fadeev, A. Y.; McCarthy, T. J. Self-assembly is not the only reaction possible between alkyltrichlorosilanes and surfaces: Monomolecular and oligomeric covalently attached layers of dichloro- and trichloroalkylsilanes on silicon. *Langmuir* **2000**, *16* (18), 7268–7274.

(54) Boukherroub, R.; Petit, A.; Loupy, A.; Chazalviel, J. N.; Ozanam, F. Microwave-assisted chemical functionalization of hydrogen-terminated porous silicon surfaces. *J. Phys. Chem. B* **2003**, *107* (48), 13459–13462.

(55) (a) Love, J. C.; Estroff, L. A.; Kriebel, J. K.; Nuzzo, R. G.; Whitesides, G. M. Self-Assembled Monolayers of Thiolates on Metals as a Form of Nanotechnology. *Chem. Rev.* **2005**, *105* (4), 1103–1170. (b) Niklewski, A.; Azzam, W.; Strunskus, T.; Fischer, R. A.; Woll, C. Fabrication of self-assembled monolayers exhibiting a thiol-terminated surface. *Langmuir* **2004**, *20* (20), 8620–8624. (c) Jiang, W.; Zhitenev, N.; Bao, Z.; Meng, H.; Abusch-Magder, D.; Tennant, D.; Garfunkel, E. Structure and Bonding Issues at the Interface between Gold and

Self-Assembled Conjugated Dithiol Monolayers. *Langmuir* **2005**, *21* (19), 8751–8757.

(56) (a) Fenter, P.; Eisenberger, P.; Liang, K. S. Chain-Length Dependence of the Structures and Phases of Ch3(Ch2)N-1sh Self-Assembled on Au(111). *Phys. Rev. Lett.* **1993**, *70* (16), 2447–2450. (b) Porter, M. D.; Bright, T. B.; Allara, D. L.; Chidsey, C. E. D. Spontaneously Organized Molecular Assemblies 0.4. Structural Characterization of Normal-Alkyl Thiol Monolayers on Gold by Optical Ellipsometry, Infrared-Spectroscopy, and Electrochemistry. *J. Am. Chem. Soc.* **1987**, *109* (12), 3559–3568.

(57) Aliganga, A. K. A.; Duwez, A. S.; Mittler, S. Binary mixtures of self-assembled monolayers of 1,8-octanedithiol and 1-octanethiol for a controlled growth of gold nanoparticles. *Org. Electron.* **2006**, *7* (5), 337–350.

(58) Gergel-Hackett, N.; Zangmeister, C. D.; Hacker, C. A.; Richter, L. J.; Richter, C. A. Demonstration of molecular assembly on Si (100) for CMOS-compatible molecule-based electronic devices. *J. Am. Chem. Soc.* **2008**, *130* (13), 4259–4261.

(59) Brown, K. E.; Dlott, D. D. High-Pressure Raman Spectroscopy of Molecular Monolayers Adsorbed on a Metal Surface. *J. Phys. Chem. C* **2009**, *113* (14), 5751–5757.

(60) (a) Kondoh, H.; Nambu, A.; Ehara, Y.; Matsui, F.; Yokoyama, T.; Ohta, T. Substrate dependence of self-assembly of alkanethiol: X-ray absorption fine structure study. *J. Phys. Chem. B* **2004**, *108* (34), 12946–12954. (b) Tivanski, A. V.; Li, J. K.; Walker, G. C. Pressure-induced restructuring of a monolayer film nanojunction produces threshold and power law conduction. *Langmuir* **2008**, *24* (6), 2288–2293.

(61) Boukherroub, R. Chemical reactivity of hydrogen-terminated crystalline silicon surfaces. *Curr. Opin. Solid State Mater. Sci.* **2005**, *9* (1−2), 66–72.

(62) Eves, B. J.; Sun, Q. Y.; Lopinski, G. P.; Zuilhof, H. Photochemical attachment of organic monolayers onto H-terminated Si(111): Radical chain propagation observed via STM studies. *J. Am. Chem. Soc.* **2004**, *126* (44), 14318–14319.

(63) (a) Hacker, C. A.; Batteas, J. D.; Garno, J. C.; Marquez, M.; Richter, C. A.; Richter, L. J.; van Zee, R. D.; Zangmeister, C. D. Structural and chemical characterization of monofluoro-substituted oligo-(phenylene-ethynylene) thiolate self-assembled monolayers on gold. *Langmuir* **2004**, *20* (15), 6195–6205. (b) Cornil, J.; Karzazi, Y.; Brédas, J. L. Negative Differential Resistance in Phenylene Ethynylene Oligomers. *J. Am. Chem. Soc.* **2002**, *124* (14), 3516–3517. (c) Logdlund, M.; Salaneck, W. R.; Meyers, F.; Bredas, J. L.; Arbuckle, G. A.; Friend, R. H.; Holmes, A. B.; Froyer, G. Evolution of the Electronic-Structure in a Conjugated Polymer Series - Polyacetylene, Poly(P-Phenylene), and Poly(P-Phenylenevinylene). *Macromolecules* **1993**, *26* (15), 3815–3820.

(64) (a) Arnold, R.; Terfort, A.; Woll, C. Determination of molecular orientation in self-assembled monolayers using IR absorption intensities: The importance of grinding effects. *Langmuir* **2001**, *17* (16), 4980–4989. (b) Vance, A. L.; Willey, T. M.; Nelson, A. J.; van Buuren, T.; Bostedt, C.; Terminello, L. J.; Fox, G. A.; Engelhard, M.; Baer, D. XAS and XPS Characterization of Monolayers Derived from a Dithiol and Structurally Related Disulfide-Containing Polyamides. *Langmuir* **2002**, *18* (21), 8123–8128.

(65) Tour, M. J.; Jones, L., II; Pearson, D. L.; Lamba, J. J. S.; Burgin, T. P.; Whitesides, G. M.; Allara, D. L.; Parikh, A. N.; Atre, S. V. Self-Assembled Monolayers and Multilayers of Conjugated Thiols, α,ω-Dithiols, and Thioacetyl-Containing Adsorbates.Understanding Attachments between Potential Molecular Wires and Gold Surfaces. *J. Am. Chem. Soc.* **1995**, *117*, 9529–9534.

(66) (a) Tao, F.; Wang, Z. H.; Lai, Y. H.; Xu, G. Q. Attachment of styrene and phenylacetylene on si(111)-7 × 7: The influence of substitution groups on the reaction mechanism and formation of pi-conjugated skeletons. *J. Am. Chem. Soc.* **2003**, *125* (22), 6687–6696. (b) Schwartz, M. P.; Ellison, M. D.; Coulter, S. K.; Hovis, J. S.; Hamers, R. J. Interaction of pi-conjugated organic molecules with pi-bonded semiconductor surfaces: Structure, selectivity, and mechanistic implications. *J. Am. Chem. Soc.* **2000**, *122* (35), 8529–8538.

(67) Coulter, S. K.; Schwartz, M. P.; Hamers, R. J. Sulfur atoms as tethers for selective attachment of aromatic molecules to silicon(001) surfaces. *J. Phys. Chem. B* **2001**, *105* (15), 3079–3087.

(68) (a) Salomon, A.; Boecking, T.; Seitz, O.; Markus, T.; Amy, F.; Chan, C.; Zhao, W.; Cahen, D.; Kahn, A. What is the barrier for tunneling through alkyl monolayers? Results from n- and p-Si-Alkyl/Hg junctions. *Adv. Mater.* **2007**, *19* (3), 445–450. (b) Thieblemont, F.; Seitz, O.; Vilan, A.; Cohen, H.; Salomon, E.; Kahn, A.; Cahen, D. Electronic Current Transport through Molecular Monolayers: Comparison between Hg/Alkoxy and Alkyl Monolayer/Si(100) Junctions. *Adv. Mater.* **2008**, *20* (20), 3931–3936. (c) Yaffe, O.; Scheres, L.; Puniredd, S. R.; Stein, N.; Biller, A.; Lavan, R. H.; Shpaisman, H.; Zuilhof, H.; Haick, H.; Cahen, D.; Vilan, A. Molecular Electronics at Metal/Semiconductor Junctions. Si Inversion by Sub-Nanometer Molecular Films. *Nano Lett.* **2009**, *9* (6), 2390–2394.

(69) (a) Mahapatro, A. K.; Scott, A.; Manning, A.; Janes, D. B. Gold surface with sub-nm roughness realized by evaporation on a molecular adhesion monolayer. *Appl. Phys. Lett.* **2006**, *88* (15), 3. (b) Hsu, J. W. P.; Loo, Y. L.; Lang, D. V.; Rogers, J. A. Nature of electrical contacts in a metal-molecule-semiconductor system. *J. Vac. Sci. Technol. B* **2003**, *21* (4), 1928–1935.

(70) (a) Vilan, A.; Yaffe, O.; Biller, A.; Salomon, A.; Kahn, A.; Cohen, D. Molecules on Si: Electronics with Chemistry. *Adv. Mater.* **2010**, *22* (2), 140–159. (b) Stein, N.; Korobko, R.; Yaffe, O.; Har Lavan, R.; Shpaisman, H.; Tirosh, E.; Vilan, A.; Cahen, D. Nondestructive Contact Deposition for Molecular Electronics: Si-Alkyl//Au Junctions. *J. Phys. Chem. C* **2010**, *114* (29), 12769–12776. (c) Salomon, A.; Backing, T.; Gooding, J. J.; Cahen, D. How Important Is the Interfacial Chemical Bond for Electron Transport through Alkyl Chain Monolayers?. *Nano Lett.* **2006**, *6* (12), 2873–2876.

(71) Beebe, J. M.; Kim, B.; Gadzuk, J. W.; Frisbie, C. D.; Kushmerick, J. G. Transition from direct tunneling to field emission in metal-molecule-metal junctions. *Phys. Rev. Lett.* **2006**, *97* (2), 026801.

(72) Salomon, A.; Boecking, T.; Chan, C. K.; Amy, F.; Girshevitz, O.; Cahen, D.; Kahn, A. How do electronic carriers cross Si-bound alkyl monolayers?. *Phys. Rev. Lett.* **2005**, *95* (26), 266807.

(73) Salomon, A.; Cahen, D.; Lindsay, S.; Tomfohr, J.; Engelkes, V. B.; Frisbie, C. D. Comparison of electronic transport measurements on organic molecules. *Adv. Mater.* **2003**, *15* (22), 1881–1890.

(74) Detailed analysis of the $I-V$ curves between 0 and 0.2 V performed by using the thermionic emission model showed minimal differences in the ideality factor (n) and the barrier energy ($q\varphi$) for all four molecules. (See Supporting Information.)

(75) Akkerman, H. B.; de Boer, B. Electrical conduction through single molecules and self-assembled monolayers. *J. Phys.: Condens. Matter* **2008**, *20* (1), 013001–013021.

(76) (a) Hacker, C. A. Modifying electronic properties at the silicon-molecule interface using atomic tethers. *Solid-State Electron.* **2010**, *54* (12), 1657–1664. (b) Scott, A.; Risko, C.; Valley, N.; Ratner, M. A.; Janes, D. B. Molecular modulation of Schottky barrier height in metal-molecule-silicon diodes: Capacitance and simulation results. *J. Appl. Phys.* **2010**, *107*, 2.

(77) (a) Himpsel, F. J.; Hollinger, G.; Pollak, R. A. Determination of the Fermi-Level Pinning Position at Si(111) Surfaces. *Phys. Rev. B* **1983**, *28* (12), 7014–7018. (b) Monch, W. *Semiconductor Surfaces and Interfaces*; Springer-Verlag: Berlin, 1993.

(78) Bent, S. F. Heads or Tails: Which Is More Important in Molecular Self-Assembly?. *Acs Nano* **2007**, *1* (1), 10–12.

(79) Segev, L.; Salomon, A.; Natan, A.; Cahen, D.; Kronik, L.; Amy, F.; Chan, C. K.; Kahn, A., Electronic structure of Si(111)-bound alkyl monolayers: Theory and experiment. *Phys. Rev. B* **2006**, *74* (16), -.

(80) Yu, L. H.; Gergel-Hackett, N.; Zangmeister, C. D.; Hacker, C. A.; Richter, C. A.; Kushmerick, J. G. Molecule-induced interface states dominate charge transport in Si-alkyl-metal junctions. *J. Phys.: Condens. Matter* **2008**, *20* (37), 5.

(81) (a) Scott, A.; Janes, D. B. Gold/Molecule/p(+) Si Devices: Variable Temperature Electronic Transport. *IEEE Trans. Nanotechnol.* **2010**, *9* (4), 494–503. (b) Engelkes, V. B.; Beebe, J. M.; Frisbie, C. D.

Length-dependent transport in molecular junctions based on SAMs of alkanethiols and alkanedithiols: Effect of metal work function and applied bias on tunneling efficiency and contact resistance. *J. Am. Chem. Soc.* **2004**, *126* (43), 14287–14296.

(82) van der Marel, C.; Yidirim, M.; Stapert, H. R. Multilayer approach to the quantitative analysis of x-ray photoelectron spectroscopy results: Applications to ultrathin SiO2 on Si and to self-assembled monolayers on gold. *J. Vac. Sci. Technol. A* **2005**, *23* (5), 1456–1470.